Supplementary File S1

Determination of aluminum abundance in brain tissues using electrothermal atomic-absorption spectrometry (ETAAS) - Tissues were harvested under RNAse-free clean conditions and were subjected to Zeeman-type ETAAS trace metal analysis for aluminum typically most tissue samples were 0.5 gm wet weight. All human tissues, chemicals and reagents, protein extraction and quality control and all analytical and ultrapure chemicals and reagents used in these experiments were obtained from standard commercial suppliers; all chemicals and reagents were used in accordance with the manufacturer's specifications and without any additional purification.

Aluminum analysis and ETAAS Sample Preparation - Individual tissues were dissected free of connective tissue and vasculature and washed briefly in ultrapure water (18 megohm, Millipore or Puriss 95305, Milli-Q water; Fluka; Tracepur® product 1.00473 EMD Merck-Millipore Bellerica MA, USA; aluminum content <1 ppb); samples were next 'dry' ashed in platinum mini-crucibles, taken up in concentrated ultrapure HNO_3 (OmniTrace UltraTM Nitric acid NX0408, EMD Merck-Millipore, or ULTREX II Ultrapure Reagent, JT Baker/VWR Radnor PA, USA; aluminum content ~20 ppt) and subjected to ETAAS as previously described by our laboratory and others. Parallel sets of samples were also analyzed using the 'wet'-digestion method of Trapp et al (1978) and Van der Voet (1985) as modified by van Ginkel et al., (1990) [**S1-S3**]. In the later method 0.5 gm samples of tissue in disposable polypropylene or Teflon tubes were incubated 24 hr at 45^{o}C in 0.8 mL concentrated ultrapure nitric acid and 0.2 ml concentrated ultrapure sulfuric acid (ULTREX II Ultrapure Reagent, J.T.Baker/VWR Radnor PA, USA; aluminum content <50 ppt) in a dedicated 24 position thermomixer/extractor device (Eppendorf model 5436; Eppendorf Inc, Hauppauge NY, USA) with constant agitation; the temperature was next raised to 70^{o}C for 3 hrs and then 105^{o}C resulting in a clear yellow solution, diluted up to 3.0 ml with ultrapure water and subjected to trace metal analysis. The use of a dedicated thermomixer device with constant agitation at elevated temperature ensured a thorough concentrated acid-based dissolution of the sample (as suggested by the manufacturer of OmniTrace UltraTM acids; such as Nitric acid NX0408, EMD Merck-Millipore). In either sample hysdrolysis method there was no particulate matter visible in the hydrolysate solution. All sample tubes were spun briefly in a table top microfuge to make sure all liquid in the vial was drained from the seal and the sides of the walls of the analytical tubes prior to analysis.

Analytical Parameters, controls and independent analysis - Trace metal analysis was performed in triplicate or quadruplicate on 20 uL samples using electrothermal atomic absorption spectrophotometry (ETAAS); PE5000PC system, Zeeman-type, Perkin-Elmer, Waltham MA, USA) equipped with an PE automated sampler (18 and 24 position autosampler; aluminum detection limit ~2.2 ng/mL) and an IBM/AT supported analysis package for trace metal analysis, as previously described by our group and others. For multiple sample analyses data were obtained as 'relative signal strength' of aluminum abundance to a standard, or aluminum expressed as ng/gm or ug/gm wet weight of tissue. The ETAAS device hollow-cathode lamp was operated at 15 mA; atomic absorption for aluminum was measured at 309.3 nm with a spectral band width of 0.7 nm; the purge gas was Argon at 300 ml/min gas flow; gas flow was interrupted at atomization; typically the dry cycle was 130^{o}C, 10 sec ramp, 5 sec hold; char cycle 1500^{o}C, 18 sec ramp with a 6 sec hold; the atomize cycle was 2700^{o}C with a 0 sec ramp and a 6 sec hold, although other programs were used with quantitatively similar results; aluminum concentrations in the digest were determined using the standard addition method. In the later a 10 mg/L aluminum aqueous solution was prepared from ultrapure

reagents; aqueous standard solutions of 0, 10, 20 and 50 ug/L were prepared; typically a 250 uL sample of digest was mixed with an equal volume of standard solution prior to analysis in duplicate; the detection limit of this assay was about 5.0 ng aluminum/gm wet weight of tissue. Some samples were also analyzed using an X-ray-fluorescence raster-scanning (XRFR) spectroscopy device at the advanced photon source (APS) facility at Argonne National Laboratories, US Department of Energy, University of Chicago (by authors B. Lai, W.J. Lukiw, S. Vogt, W. Walsh) with similar results and patterns of nuclear tissue accumulation of aluminum. The APS XRFR technique is the most sensitive ever devised for trace metal analysis in biological thin-sections, is of an experimental nature and is still under development (see **Supplementary File S4**).

Statistical analysis, data interpretation and integrated bioinformatics analysis

For ETAAS data analysis all statistical procedures were analyzed using (*p*, ANOVA) a two-way factorial analysis of variance using algorithms and procedures in the SAS language (Statistical Analysis Institute, Cary, NC, USA). In the results *p*-values of less than 0.05 (ANOVA) were considered to be statistically significant. All aluminum data were collected and analyzed using Excel 2016 (Office 365) algorithms (Microsoft Corporation, Redmond WA, USA); all figures were generated using Adobe Illustrator CC 2015 and Photoshop CC version14.0 (Adobe Corporation, San Jose CA, USA). Additional data and figures were displayed using Excel 2008 (Microsoft Corporation, Redmond WA), Adobe Illustrator CS3' and as previously described [50]; see also **Supplementary File S4**.

Additional methodological details can be found in this recent publication; Pogue AI, Zhao Y, Jaber V, Percy ME, Cong L., Lukiw WJ. (2017) systemic inflammation in C57BL/6J mice receiving dietary aluminum sulfate; up-regulation of the pro-inflammatory cytokines IL-6 and TNFα, C-reactive protein (CRP) and miRNA-146a in blood serum, Journal of Neurology and Neurotoxicology 1:1 NIHMSID 932901; http://www.sciaeon.org/articles/JNNT-1-001.pdf.

References for Supplementary File S1

[S1] Trapp GA, Miner GD, Zimmerman RL, Mastri AR, Heston LL. Aluminum levels in brain in Alzheimer's disease. Biol Psychiatry. 1978 Dec;13(6):709-18. PubMed PMID: 737258.

[S2] van der Voet GB, de Haas EJ, de Wolff FA. Monitoring of aluminum in whole blood, plasma, serum, and water by a single procedure using flameless atomic absorption spectrophotometry. J Anal Toxicol. 1985 May-Jun;9(3):97-100. PubMed PMID: 4010240.

[S3] van Ginkel MF, van der Voet GB, de Wolff FA. Improved method of analysis for aluminum in brain tissue. Clin Chem. 1990 Apr;36(4):658-61. PubMed PMID: 2323045.

SUPPLEMENTARY FILE 2

Raw Data

aluminum	AD	ACG	ASD	YCG	AFT	ALS	DDS	DS	HC	MID
1	3.7	1.5	1	1	0.9	1.1	3.3	4.3	1.6	1.7
2	4.8	1.4	1.1	1.5	1.05	1.3	4.1	3	2.9	1.3
3	6.1	1.5	1.2	0.9	1.3	1.05	2.7	4.6	0.5	1.2
4	3.6	1.3	1.6	1.1	1.4	1	4.7	2	1.7	1.15
5	3.8	1.6	1.3	1	1.1	1.2	3.5	6.5	3.1	1.4
6	9.4	1.3	1.4	1.3	1.15	1.25	3.9	4.1	0.3	1.5
7	8.3	1.25	1.1	1.4		1.35	4.2	4.5	1.8	2
8	6.1	1.45	0.9	1.1		1.15	3.2	5.1	2.7	1.4
9	4.7	1.5	0.95	1.2		1.3	4.1	6.1	0.7	1.7
10	3.65	1.6	1.1	1.3		1.2	3.3	4.9	1.7	1.2
11	7.1	1.8	1.6	1.2		1.3	2.9	4.2	1.2	1.1
12	12.5	1.4	1.5	1.2		1.3	3.4	4.1	1.7	2.05
13	6.7	1.45	1.2	1.5		1.4	4	4.8	2	1.1
14	5.9	1.5	1.2	0.9		0.95	2.7	7.1	1	1.2
15	5.2	1.6	1.5	1.5		1.4	2.2	3.5	2.4	1.2
16	9.45	1.75	1.4	1.3		1.25	5.2	4.5		1.1
17	4.5	1.4	1.3	1.1			5.4	3.9		1
18	4.6	1.2	1.2	1.2			1.2	5.1		1.3
19	10.3	1.35	1.2	0.9			1.7	4.5		1.1
20	4.75	1.6	1.3	1.1			6.2	4.9		
21	8.5	1.3	1.4	1.2			3.5	4.9		
22	6.5	0.9	0.95	1.4			2.5	5.5		
23	12.5	1.1	0.95				4.9	4.5		
24	5.9	0.95	1.2				3.7	2		
25	9.6	1.1	1.15				3.9			
26	5.1	0.85	1.05				4.7			
27	4.5	1.2					4.5			
28	2.1	1.3								
29	2.05	1.35								
30	6.9	1.4								
31	8.4	1.45								
32	9.3	1.25								
33	1.9	1.65								
34	2.1	0.16								
35	5.9	1.5								
36	4.85	1.8								
37	8.9	1.2								
38	9.5	1.1								
39	8.7	1.3								
40	12.4	1.35								
41	9.6	1.4								
42	10.1	1.35								
43	9.8	1.4								
44	10.3	1.2								
45	8.7	1.1								
46	5.5	1.4								
47	8.1	1.8								
48	9.7	1.75								
49	8.7	1.3								
50	6.8	1.25								
51	10.5	1.15								
52	11.4	1.2								
53	7.8	0.95								
54	7.5									
55	8.4									
56	8.8									
57	9.3									

58	7.2
59	6.9
60	9.1
61	8.9
62	7.6
63	10.7
64	7.9
65	6.5
66	7.3
67	5.9
68	8.9
69	7.6
70	11.8
71	10.5
72	11.4
73	9.3
74	15.5
75	16.8
76	12.5
77	12.2
78	11.6
79	6.5
80	8.9
81	9.7
82	9.9
83	11.7
84	10.8
85	9.4
86	7.9
87	6.6
88	7.5
89	6.8
90	7.6
91	11.8
92	8.1
93	14.5
94	9.3
95	7.5
96	12.4
97	6.7
98	12.1
99	2.05
100	5.9
101	15.6
102	9.2
103	11.9
104	10.2
105	11.1
106	9.7
107	8.1
108	10.4
109	9.4
110	7.2
111	9.1
112	8.1
113	9.7
114	7.2
115	11.6
116	10
117	13.6
118	9.3
119	6.5

120	8.1
121	8.5
122	8.5
123	9.6
124	10.1
125	8.9
126	11
127	10.7
128	9.4
129	8.4
130	11.3
131	7.3
132	5.8
133	4.5
134	3.9
135	6.7
136	7.5
137	8.4
138	5.7
139	9.6
140	12.4
141	15.1
142	3.9
143	10.5
144	9.5
145	10.2
146	8.7
147	7.2
148	5.8
149	11.1
150	7.2
151	6.4
152	5.4
153	2.1
154	5.5
155	2.6
156	5.2
157	7.4
158	8.4
159	15.3
160	4.7
161	7.2
162	5.6
163	6.5
164	4.8
165	6.2
166	2.3
167	5.6
168	7.8
169	13.5
170	6.5
171	7.2
172	5.5
173	10.2
174	3.8
175	6.9
176	5.8
177	6.5
178	5.7
179	3.6
180	6.8
181	3.9

182	**7.4**
183	**6.8**
184	**9.4**
185	**10.5**
186	**9.4**

MS	PD	PrD	PML	PSP	SCZ
1.1	1.6	1.5	1.1	1.2	1.05
0.9	0.6	0.9	1.9	0.9	2.1
1.05	2.1	0.95	1	1.3	2
1.8	3	2.1	2.2	1.45	1
1.4	1.2	1.4	2	1.45	2.3
1.3	2.4	1.5	1.4	2.3	1.2
1.1	1.7	1.2	1.5	1.9	1.6
0.95	1.8	1.1	0.7	1.45	1.4
2.1	1.1	1.2	2.3	2.05	1.5
1.8	2.5	1.5	1.6	1.6	2
1.9	2	1.1	0.8	1.25	1.7
1.5	1.8			1.6	1.45
1.1	1.5			1.65	0.7
0.8	1.8			1.6	1.5
2.1	1.9			1.45	2.4
1.8	1.6			0.85	2.5
1.2	0.6			1.75	2
1.1	2			1.5	1.1
1.4	0.4			0.5	2.7
1.3	2.2			1.9	2.4
0.7	1.8			1.3	1.9
1.1	2.5			0.95	
2.1	1.1			1.6	
	3.2			1.4	
	0.4				
	2				
	3				

Supplementary File S3

DISEASE		WEBSITE
Alzheimer's disease	AD	https://www.nia.nih.gov/health/alzheimers-disease-fact-sheet
Ataxia Friedreichs-type	AFT	https://www.ninds.nih.gov/Disorders/Patient-Caregiver-Education/Fact-Sheets/Friedreichs-Ataxia-Fact-Sheet
amyotrophic lateral sclerosis	ALS	https://www.ninds.nih.gov/Disorders/Patient-Caregiver-Education/Fact-Sheets/Amyotrophic-Lateral-Sclerosis-ALS-Fact-Sheet
autism spectrum disorder	ASD	https://www.ninds.nih.gov/Disorders/Patient-Caregiver-Education/Fact-Sheets/Autism-Spectrum-Disorder-Fact-Sheet
dialysis dementia syndrome	DDS	https://report.nih.gov/nihfactsheets/ViewFactSheet.aspx?csid=34
Down's syndrome (trisomy 21)	DS	(DS) https://www.nichd.nih.gov/health/topics/down/conditioninfo
Huntington's chorea	HC	https://www.ninds.nih.gov/Disorders/All-Disorders/Huntingtons-Disease-Information-Page
multiple infarct dementia	MID	https://www.ninds.nih.gov/disorders/all-disorders/multi-infarct-dementia-information-page
multiple sclerosis	MS	https://report.nih.gov/NIHfactsheets/ViewFactSheet.aspx?csid=103
Parkinson's disease	PD	https://www.ninds.nih.gov/Disorders/All-Disorders/Parkinsons-Disease-Information-Page; https://report.nih.gov/NIHfactsheets/ViewFactSheet.aspx?csid=109
prion disease (includes BSE, CJD, GSS)	PrD	https://www.ninds.nih.gov/Disorders/Patient-Caregiver-Education/Fact-Sheets/Creutzfeldt-Jakob-Disease-Fact-Sheet; https://www.ninds.nih.gov/Disorders/Patient-Caregiver-Education/Fact-Sheets/Creutzfeldt-Jakob-Disease-Fact-Sheet-Healthcare
progressive multifocal leukoencephalopthy	PML	progressive multifocal leukoencephalopthy (PML) https://www.ninds.nih.gov/Disorders/All-Disorders/Progressive-Multifocal-Leukoencephalopathy-Information-Page
progressive supranuclear palsy	PSP	https://www.ninds.nih.gov/Disorders/Patient-Caregiver-Education/Fact-Sheets/Progressive-Supranuclear-Palsy-Fact-Sheet
schizophrenia	SCZ	https://report.nih.gov/nihfactsheets/ViewFactSheet.aspx?csid=67

Supplementary file S4

Figure S4-1: Argonne National Laboratory's Advanced Photon Source (APS)

Figure S4-1: Argonne National Laboratory's Advanced Photon Source (APS) - Located at the Argonne-National-Laboratory, US Department of Energy (US DOE), University of Chicago IL, USA, the Advanced Photon Source (APS) is a national synchrotron-radiation light source research facility and was the location of the 7 GeV X-ray-fluorescence raster-scanning (XRFR) spectroscopy experiments still in progress. The APS produces the world's most brilliant X-ray beam of 7 GeV energies and higher (classified information by the US DOE). Experimental suites are located around the perimeter of the 1.4 kilometer diameter ring at tangents to the main accelerator ring; the experiments described here used undulator-beam-line 2-ID-E (https://www.aps.anl.gov/; last accessed 1 December 2018).

Figure S4-2: Schematic Drawing of the APS

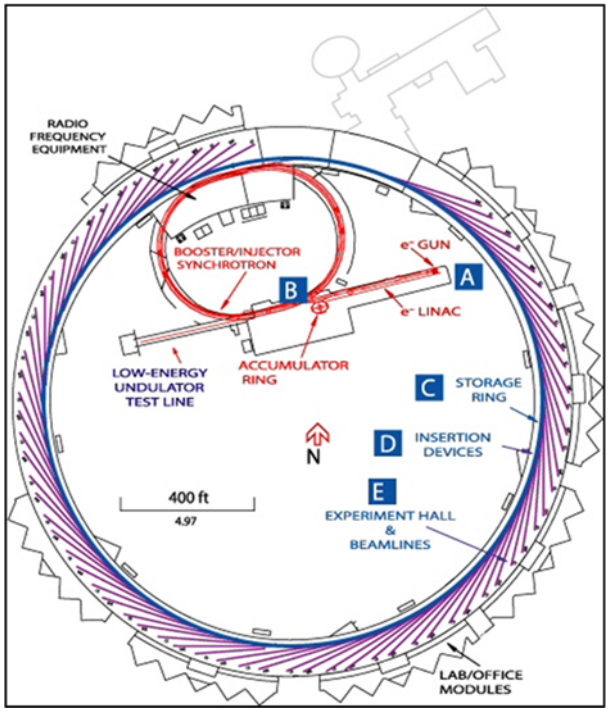

Figure S4-2: Schematic Drawing of the APS - Schematic showing the basic design and experimental suites containing analytical apparatus including some details of the undulator-beam-line 2-ID-E at the APS (white 'E' in blue box).

Figure S4-3: Novel X-Ray fluorescence Raster (XRFR) Spectroscopy Scanning System Detector

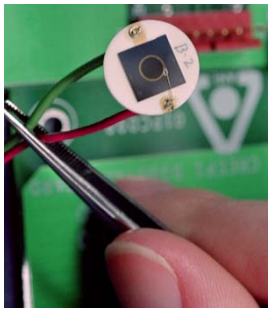

Figure S4-3: Novel X-Ray fluorescence Raster (XRFR) Spectroscopy Scanning System Detector - The silicon-nitride (SiN) window configuration for determining trace metal abundance in biological materials; the central circular SiN window on the XRFR B-2 sensor is about 3 mm in diameter on which unstained 10 um micro thick brain tissue samples are overlain.

Figure S4-4: Typical Multi-Element XRFR Spectra

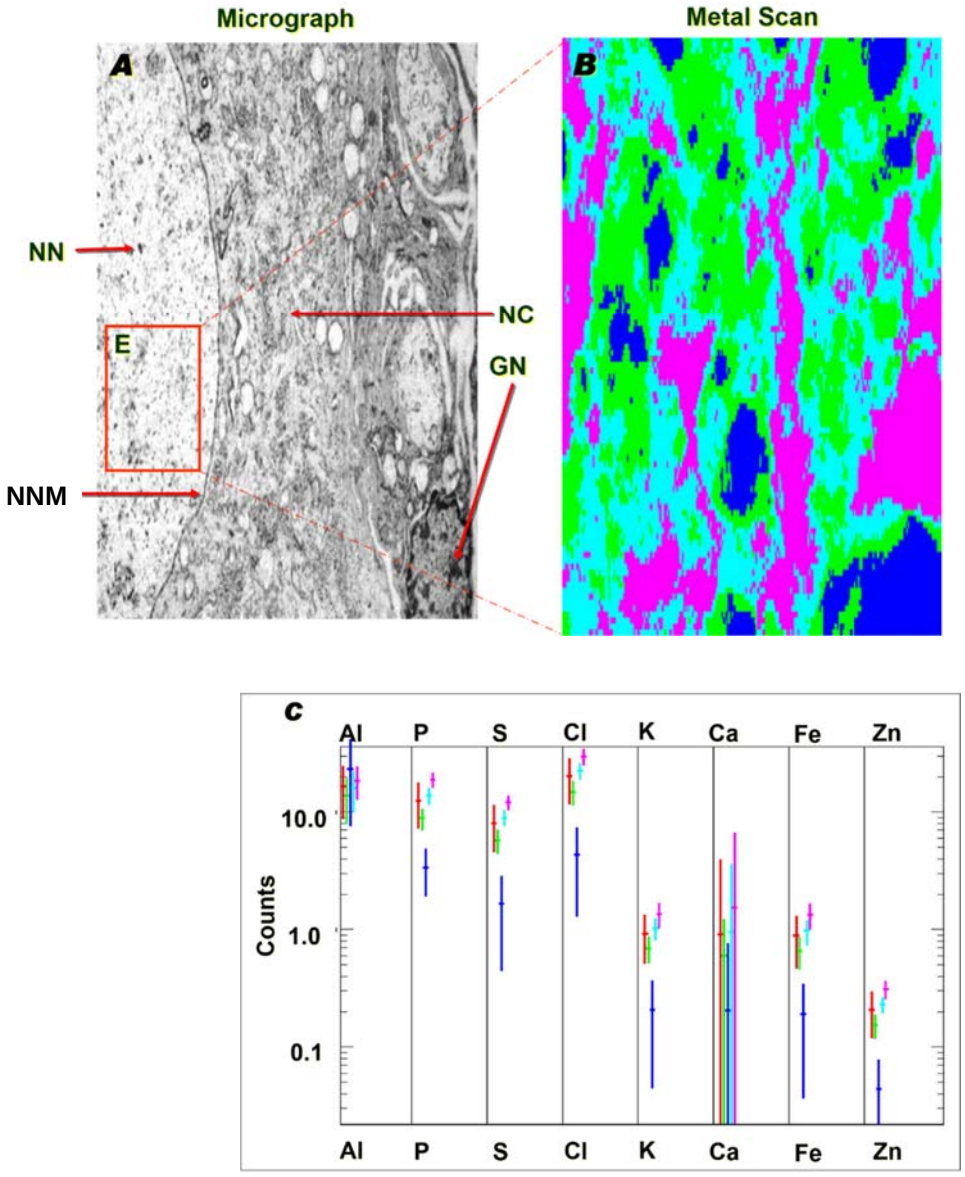

Figure S4-4: Typical Multi-Element XRFR Spectra - Multi-element XRFR spectra using an energy dispersive germanium detector (Ultra-LEGe, Canberra Instruments, Meriden CT, USA); **(A)** electron micrograph of scanned tissue; (dimensions, 4x8 micron); showing neuronal nucleus (NN); glial nucleus (GN); neuronal cytoplasm (NC); neuronal nuclear membrane (NNM); boxed area 'E' shown expanded at right for (B) 'Metal Scan'; **(B)** Metal scan of euchromatin **(E)** region in **(A)** (dimensions 1x2 micron). **(C)** Panel **C** shows the relative signal strength for Al, P, S, Cl, K, Ca, Fe and Zn in the '**E'** sub-region of NN from an Alzheimer's disease (AD) affected brain compared to the same regions of an age-, gender- and PMI-matched control.

Figure S4-5: Typical Multi-Element XRFR Scanning Spectra in Control and Alzheimer Brain Nuclei

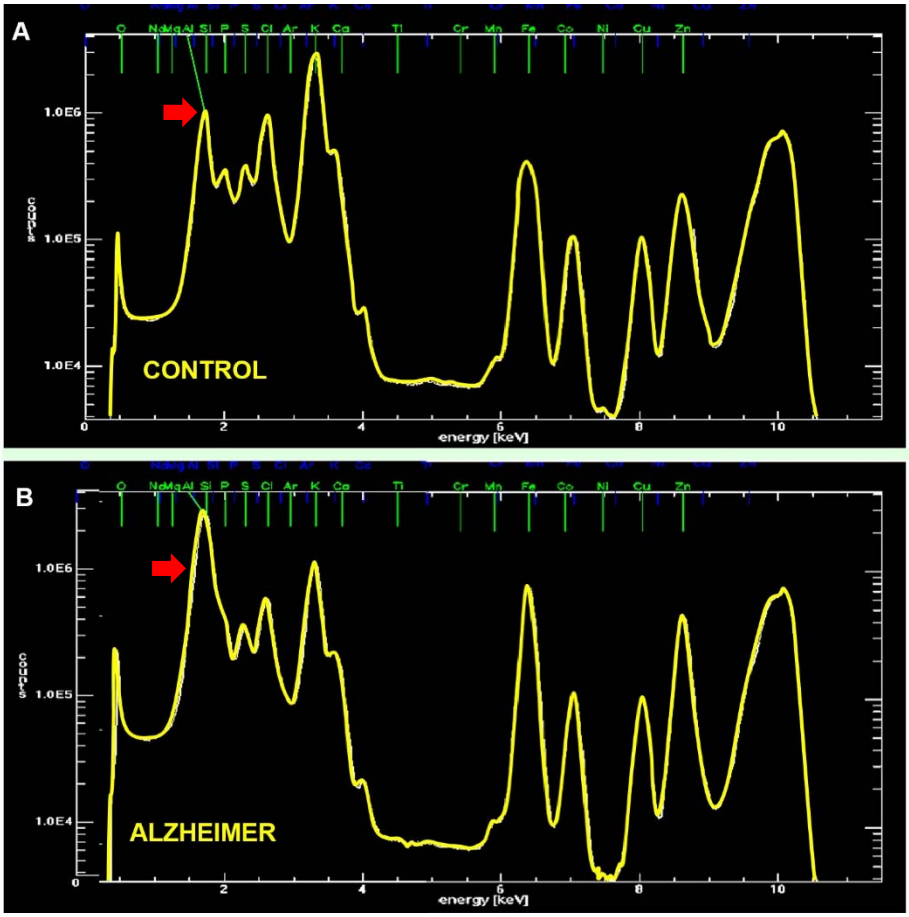

Figure S4-5: Typical Multi-Element XRFR Scanning Spectra in Control and Alzheimer Brain Nuclei - Multi-element XRFR spectra in control and Alzheimer brain nuclei; **(A)** Association neocortical nuclear scan from Brodmann area A22, superior temporal lobe, of a cognitively normal 72 year-old female; post-mortem interval (PMI) 2.1 hr; **(B)** Association neocortical nuclear scan from Brodmann area A22, superior temporal lobe, of an Alzheimer's disease affected 72 year-old female; post-mortem interval (PMI) 2.3 hr; significant increases in the abundance of Al^{3+} can be seen in the AD versus control brain (red arrow); note logarithmic scale on the ordinate (y-axis); other trace metal abundances that showed smaller changes included those for K^{+}, Cl^{-}, Fe^{2+} and Si^{4+}**.**

Preliminary Findings using the XRFR method: This novel analytical technique is still under development and the use of the APS facility is highly restricted to qualified scientific, medical and military researchers. To date our group has focused on the analysis of Alzheimer (AD; N=3; mean age 74.5+/-8.4 yrs) and control (no neurological disease; N=3; mean age 73.8+/-7.5 yrs) tissue samples. As indicated above; this technology is capable of detecting Al, P, S, Cl, K, Ca, Fe and Zn non-destructively in ultra-thin-10-um-sections of human-brain tissue samples in extremely complex biological-samples (see **Figure S4-3** to **S4-5** above); each ultra-thin-10-um-sectioned human-brain tissue sample is typically scanned in triplicate; ~3.8 million separate-elemental-analyses were achieved in a ~4-day experiment; to date we have collected about $7x10^9$ data points amenable to ongoing bioinformatics and biostatistical analysis; in agreement with the ETAAS results these preliminary data indicate that using XRFR we have found a major increase in aluminum in AD brain to approximately 5-9-fold over age-matched control and the results are highly significant (p<000.1 (ANOVA); see also **Table 1**).